



Obrabotka metallov - Metal Working and Material Science

Journal homepage: http://journals.nstu.ru/obrabotka_metallov



Features of the superposition of ultrasonic vibrations in the welding process

Sergey Sundukov *

Moscow Automobile and Road Construction State Technical University (MADI), 64 Leningradsky prospect, Moscow, 125319, Russian Federation

 <https://orcid.org/0000-0003-4393-4471>,  sergey-lefmo@yandex.ru

ARTICLE INFO

Article history:

Received: 25 March 2022

Revised: 13 May 2022

Accepted: 15 May 2022

Available online: 15 June 2022

Keywords:

Ultrasound

Welding

Vibrations

Cavitation

Microstructure

Dendritic segregation

Funding

This research was funded by the Russian Science Foundation, grant number No. 21-79-00185, <https://rscf.ru/project/21-79-00185/>

Acknowledgements

Research was partially conducted at core facility “Structure, mechanical and physical properties of materials”

ABSTRACT

Introduction. The main problem in obtaining welded joints is the nonuniform heating of the joint zone, which leads to differences in the structure and properties of the weld metal and the base metal. One of the ways to intensify the welding process is the use of ultrasonic vibrations. As a result of the analysis of methods for introducing ultrasonic vibrations into the melting zone, a method of superimposing vibrations on the elements to be welded was chosen for experimental studies. This method makes it possible to influence the welded elements throughout the entire welding cycle from the melt bath to complete crystallization of the metal. **Methods.** Experimental studies were carried out on plates made of carbon structural steel St3 (ASTM A568M, AISI 1017, DIN 17100) and aluminum deformable non-hardened alloy AMg4 (EN AW-5086, AW-AL Mg4, 5086). As a source of oscillations, a rod magnetostrictive oscillatory system was used, the end of which was rigidly fixed on one of the welded plates. To determine the places of application of the oscillation source and the welding zone, a calculation method is proposed based on the equality of the resonant frequencies of the used oscillatory system and the natural frequency of bending vibrations of the welding component. It is shown that the optimal places for the application of vibrations and welding will be the antinodes of oscillations, which have the maximum amplitude. Welds were obtained by the method of semi-automatic gas metal arc welding. **Results and Discussion.** Microstructural study of obtained samples showed a significant decrease in the proportion of dendritic segregation. The changes in the structure are the result of the effects that occur in the liquid melt when ultrasonic vibrations are introduced. The main effects are sound pressure, cavitation and acoustical streaming. The structure change mechanism consists in the dispersion of growing dendrites and crystallization nuclei under the action of shock waves and cumulative jets that occur when cavitation bubbles collapse. The formed fragments of dendrites are new crystallization nuclei that propagate through the melt pool under the action of acoustic currents. Then the process is repeated. The resulting effects affect the kinetics of the crystallization process – the degree of supercooling increases, the number of crystallization nuclei formed per unit time increases, and the rate of its growth decreases. Changes in the structure of the weld metal lead to an increase in the quality of the welded joint, which reduces welding deformations, increases the tensile strength and significantly increases ductility.

For citation: Sundukov S.K. Features of the superposition of ultrasonic vibrations in the welding process. *Obrabotka metallov (tehnologiya, oborudovanie, instrumenty)* = *Metal Working and Material Science*, 2022, vol. 24, no. 2, pp. 50–66. DOI: 10.17212/1994-6309-2022-24.2-50-66. (In Russian).

Introduction

Welding is a key method to produce permanent joints in various machine-engineering fields. Creating stable bonds between atoms or molecules of surfaces to be joined using heating or surface plastic deformation ensures a high-quality joint of both homogeneous and heterogeneous metals and alloys and its joints with non-metallic materials [1].

Fusion welding dominates today among the existing welding types. The primary issue of this welding type is irregular heating of parts to be connected [2]. Due to the crystallization of molten and mixed base

* Corresponding author

Sundukov Sergey K., Ph.D. (Engineering), Associate Professor
Moscow Automobile and Road Construction State
Technical University (MADI)
64 Leningradsky prospect,
125319, Moscow, Russian Federation
Tel.: 8 (926) 369-19-70, e-mail: sergey-lefmo@yandex.ru

and filler metals, the weld has a cast structure. A partial melting zone of the base metal is located near the fusion boundary, which is followed by a heat-affected zone characterized by a structure changed by temperature taking place with increasing the distance from the center of the welding zone [3]. Due to structural differences, the transitions between the considered zones are accompanied by changes in mechanical properties, which is especially pronounced in the transition over the fusion boundary, which is a weak point of the weld joint.

Along with structural non-uniformity, welding issues also include residual stresses, welding deformations and weld porosity [4–7].

Various methods are used today to avoid these drawbacks that can be classified into those applied during and after welding. The methods used during welding include strain balancing by means of a reasonable sequence of weld passing, creating initial distortions and rigid fixing the elements to be welded. The methods used after welding include weld heat treatment, mechanical leveling of structures, thermal leveling, and surface plastic deformation (*SPD*) [8].

Another efficient method to minimize the consequences of these drawbacks is the vibration treatment of metal in a molten state [9–10].

This method was proposed in 1950 as applicable to crystallizing metal by *Chernov* in order to improve the ingot structure after casting. Vibrations increase the homogeneity of ingots by dispersing the growing dendrites [11–12].

To ensure efficient action on the structural formation of the weld, the crystallization of which is several times faster, it is reasonable to use high-frequency vibrations of ultrasonic frequency, which will make it possible to exert a significant impact in a limited time interval.

There are the following methods of using ultrasonic vibrations during welding:

- applying vibrations to the electrode [13];
- applying vibrations to the non-consumable electrode [14];
- transferring vibrations to the gas burner body [15];
- transferring vibrations to non-weldable structural elements [16];
- using the arch as a source of ultrasonic radiation [17].

The studies considering these methods show a positive effect on the welding process and weld structure. In particular, depending on the method, the depth of penetration of the base metal can be increased, the porosity of the weld can be decreased, the conditions for the transfer of molten metal drops from the electrode to the workpiece can be improved, the microstructure of the weld can be refined, the proportion of dendritic segregation in the weld metal can be decreased, and the mechanical properties can be improved [18–22]. More detailed results can be found in overview papers on this subject [23, 24].

The effect of ultrasonic machining on the structure of the crystallizing weld metal has a clear positive effect.

Nevertheless, these technologies are not widely used in welding processes, for example, as compared to ultrasonic *SPD* that is applied for post-treatment of welds [25–27]. This can be explained by a number of reasons:

1. Additional equipment is required: ultrasonic generator and vibration system.
2. Complex organization of the process related to coordination between welding conditions and acoustic process parameters of ultrasonic machining.
3. It is preferable to use more complex and larger magnetostrictive transducers requiring forced cooling since piezo-ceramic ones lose its efficiency at high temperatures.
4. Increased power consumption for the welding process.

Despite the difficulties, opportunities of using ultrasonic vibrations make the development of these technologies attractive.

This paper describes the research of applying ultrasonic vibrations on the elements to be welded and selecting the vibration application spot and the welding zone.

Methods

Materials

The materials widely used in welding have been selected for the study: carbon structural steel of commercial quality *St3* and deformable non-heat-treatable aluminum and magnesium alloy *AMg4*.

Welding plates were cut from a sheet workpiece 4 mm thick.

Filler materials were filler wires suitable for welding the selected materials: *Sv08Kh2GS* wire for *St3*, *ER5356* wire for *AMg4*. The wire diameter was 0.8 mm.

The chemical compositions of the materials and wires are given in Tables 1 and 2.

Table 1

Chemical composition of *AMg4* alloy and *ER5356* wire

Alloy										
Element	<i>Fe</i>	<i>Si</i>	<i>Mn</i>	<i>Cr</i>	<i>Ti</i>	<i>Cu</i>	<i>Be</i>	<i>Mg</i>	<i>Zn</i>	<i>Al</i>
%	<0.4	<0.4	0.5–0.8	0.05–0.25	0.02–0.1	<0.05	0.0002–0.005	3.8–4.8	<0.2	the rest
Filler wire										
%	<0.1	<0.25	0.55	0.12	0.12	–	–	5.0	–	the rest

Table 2

Chemical composition of steel *St3* and wire *Sv08Kh2GS*

Steel										
Element	<i>C</i>	<i>Si</i>	<i>Mn</i>	<i>Ni</i>	<i>Cr</i>	<i>Cu</i>	<i>S</i>	<i>P</i>	<i>As</i>	<i>Fe</i>
%	0.14–0.22	0.15–0.3	0.4–0.65	<0.3	<0.3	<0.3	<0.05	<0.04	<0.08	the rest
Filler wire										
%	<0.1	0.6–0.85	1.4–1.7	<0.025	1.8–2.2	<0.025	<0.015	<0.013	–	the rest

Design of experiment and equipment

The research was carried out in two stages in accordance with the design given in Fig. 1.

The first stage included welding the seam onto plates 4 mm thick and 30 mm wide followed by detecting changes in the structure of the welding zone. The second stage included welding of two plates and tension testing of the joint. The plate length was measured based on the distribution of vibration along it (as described below).

To excite vibrations in the weld zone, an ultrasonic rod vibration system comprising a magnetostrictive transducer 6 and waveguide 5 made of titanium alloy was attached to a plate 1 via threaded connection 4. The waveguide diameter was equal to the plate width (30 mm).

A *UZG 2.0/22* ultrasonic generator with frequency and amplitude adjustment was used to supply power to the vibration system. These functions maintain stable vibrations in conditions of increasing temperature and changing the volume of the plate that occur during welding.

Before welding, the plate surface was cleaned using a disc metallic brush and degreased. This was followed by ultrasonic machining and welding. Ultrasound was turned off when the weld joint cooled down to 100 °C, so that all phase transformations occurred under the influence of vibrations.

The weld was obtained by semi-automatic welding in shielding gases. Table 3 lists equipment and welding modes for *St3* and *AMg4*.

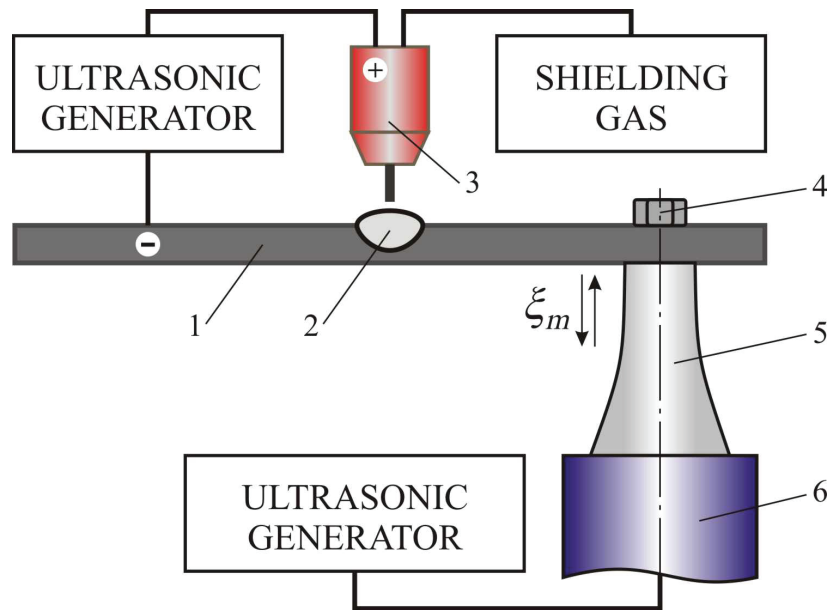


Fig. 1. Design of experiment:
 1 – plate; 2 – weld; 3 – welding torch; 4 – bolt; 5 – waveguide;
 6 – magnetostrictive transducer

Table 3

Equipment and welding modes

Welding conditions	Material	
	St3	AMg4
Welding unit type	MIG 235	MIG 215AL PULSE
Welding current I_{weld} , A	60	125
Electrical polarity	reversed	reversed
Voltage U_{weld} , V	28	22
Wire speed, V_{wire} m/min	1.9	15.2
Shielding gas	CO ₂	Ar
Shielding gas flow, l/min	8	17.5
Welding time, s	12	2

One of the most important aspects in welding with superimposed vibrations is to determine the place of its application to the plate and also the place of welding, where a stable ultrasonic effect is ensured.

Determination of vibration application and weld passing spots when using AMg4

According to the applied design of ultrasonic vibration application, the vibration system is a source of bending vibrations in the case of its normally oriented location.

In terms of process application, the optimal spot to apply vibrations will be one of the antinodes of the own vibrations of the plate. In this case, the resonance frequencies of the vibration system and the plate should be aligned.

Since a commercially available ultrasonic vibration system having a certain resonance frequency f is used in this research, the calculation is done based on the need to ensure the equal resonance frequency f_p of the plate.

The amplitude frequency response of the vibration system (Fig. 2) was taken at the end of the waveguide using a dial indicator. The resonance frequency is $f = 21,800$ Hz.

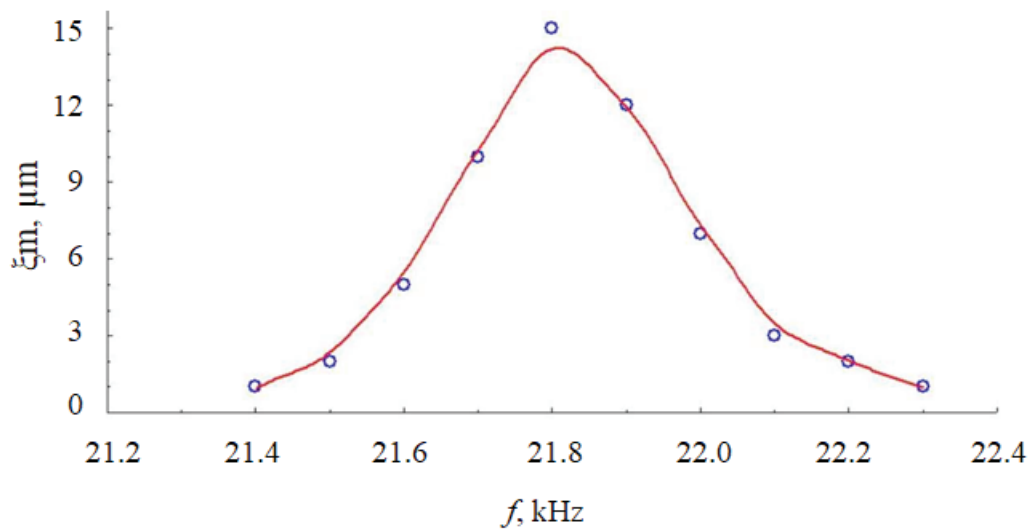


Fig. 2. Amplitude-frequency characteristic PMS-2.0-22

A differential equation for the bending vibrations of the plate [28]:

$$\frac{d^4 \xi_m}{dx^4} - \frac{\omega_0^2}{c\chi^2} \xi_m + \frac{\omega_0^2}{c^2} \frac{d^2 \xi_m}{dx^2} = 0.$$

Where ξ_m is the vibration amplitude, ω_0 is the angular frequency of self-induced vibrations, x is the plate coordinate in the longitudinal direction, c is the propagation rate of longitudinal vibrations, χ is the cross-section inertia radius.

$$\chi = \sqrt{I / S}.$$

Where I is the moment of inertia relative to the axis, S is the cross-section area.

For the rectangular plate being used (30×4 mm):

$$\chi = \sqrt{\frac{bh^3}{12}} / bh = 0.0012.$$

If the condition of $\frac{\chi^2}{l^2} \leq 0.05$ is met (0.0006 for the case under consideration), the rotary inertia can be neglected, and the equation of steady-state vibrations looks as follows:

$$\frac{d^4 \xi_m}{dx^4} - \frac{\omega_0^2}{c\chi^2} \xi_m = 0.$$

This equation was solved by Krylov (1936):

$$\xi_m = C_1 A_x + C_2 B_x + C_3 C_x + C_4 D_x,$$

where C_1, C_2, C_3, C_4 are the constants of integration that are found from boundary conditions:

$$A_x = (ch(kx) + \cos(kx)) / 2,$$

$$B_x = (sh(kx) + \sin(kx)) / 2,$$

$$C_x = (ch(kx) - \cos(kx)) / 2,$$

$$D_x = (sh(kx) - \sin(kx)) / 2.$$

To find the constants, the following equations for derivatives should be used:

$$\xi'_m = k(C_1 D_x + C_2 A_x + C_3 B_x + C_4 C_x),$$

$$\xi''_m = k^2(C_1 C_x + C_2 D_x + C_3 A_x + C_4 B_x),$$

$$\xi'''_m = k^3(C_1 B_x + C_2 C_x + C_3 D_x + C_4 A_x).$$

The factor k is the wave multiplier depending on the material properties and vibration frequency:

$$k = \sqrt[4]{\frac{m\omega^2}{EI}}, \quad (1)$$

where E is the Young modulus of the waveguide material ($E=71$ GPa for *AMg4*), m is the waveguide weight per unit of length ($m = b \cdot h \cdot l \cdot \rho = 0.03 \times 0.004 \times 1 \times 2,670 = 0.320$ kg/m for the case under consideration), angular frequency $\omega = 2\pi f_p$, where f_p is the resonance frequency of the self-induced vibrations of the plate.

To determine the nature of vibration propagation depending on the plate fixing conditions, let's use the algorithm described by *Bulgakov* (1954). Boundary conditions for this algorithm are written in expanded form, which results in heterogeneous equations relative to the constants. To avoid the constants being zero, the determinant made for the equation system coefficients should be equal to zero.

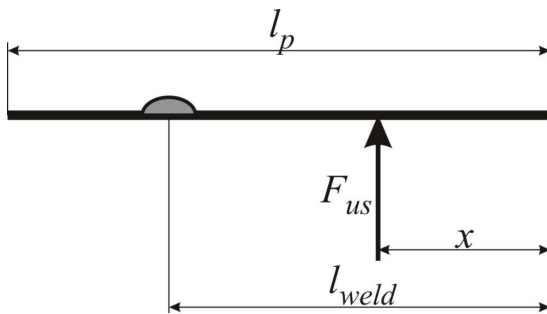


Fig. 3. Scheme for calculating bending vibrations:

l_p is the length of the plate, x is the place of ultrasonic vibrations application, l_{weld} is the place where the weld is applied

The calculation scheme is given in Fig. 3.

The ultrasonic vibration application spot x should be selected, so that in the welding zone l_{weld} there is a maximum amplitude of vibrations. For these fixing conditions (free plate ends on both sides): for $l_{sc} = 0$ and for $l_{sc} = l_p$: $\xi''_m = 0$ and $\xi'''_m = 0$, constants $C_3 = 0$ and $C_4 = 0$. Substituting these values into the solution of the vibration equation, the following frequency equation is resulted:

$$ch(kl_{II}) \cos(kl_{II}) = 1$$

The roots of the equation are:

$$kl_{II} = \pi n + \pi / 2, \quad (2)$$

where $n = 1, 2, 3 \dots$

Let's express the coefficient k from equation (2) and equate it to equation (1):

$$\frac{\pi n + \pi / 2}{l_{II}} = \sqrt[4]{\frac{m\omega^2}{EI}}.$$

Taking into account that $\omega = 2 \cdot \pi \cdot f_p$ one can obtain an equation to find the plate length depending on the vibration frequency (3):

$$l_{II} = \frac{\pi n + \pi / 2}{\sqrt[4]{\frac{m(2\pi f_n)^2}{EI}}}. \quad (3)$$

Let's calculate from the condition $f_p \approx 21,800$ Hz for various n and include the calculation values in Table 4.

Table 4

Dependence of the resonant length of the plate on n at frequency of 21,800 Hz

n	1	2	3	4	5	6	7	8
l_p	0.031	0.052	0.072	0.093	0.114	0.134	0.155	0.176
k	151.6							

Thus, the size of the plate, which provides vibrations at a resonant frequency of 21,800 Hz, corresponds to the 7th vibration mode and is 155 mm (this size was chosen for research).

The coefficient k allows associating the frequency and propagation rate of bending vibrations C_B :

$$k = \frac{\omega}{C_B},$$

where

$$C_B = \sqrt{2\pi f \chi c} = 904.5.$$

Where $c = \sqrt{\frac{E}{\rho}}$ is the rod rate of longitudinal vibrations (5,157 m/s for AMg4).

If the rate and frequency are known, the bending wavelength can be found (4):

$$\lambda_B = \frac{C_B}{f_p} = 41.3 \text{ mm} . \tag{4}$$

In this manner, when ultrasonic vibrations are communicated, the plate length fits $l_p / \lambda_B = 3.75$ bending waves. Taking into account that plate ends are free and can't have zero vibrations, let's build the diagram of vibration distributions over the plate (Fig. 4).

Vibration nodes where the amplitude is equal to zero are located at the half-wave length with a shift by 1/8 of the wave length $x_1 = (\lambda_B/2) I + \lambda_B/8$ ($I = 0, 1, 2 \dots$), and antinodes with the maximum amplitude are located at 1/4 of the wave length from nodes $x_2 = (\lambda_B/2) I + \lambda_B/8 - \lambda_B/4$. The weld locations and ultrasonic vibration application points should be selected according to distance x_2 .

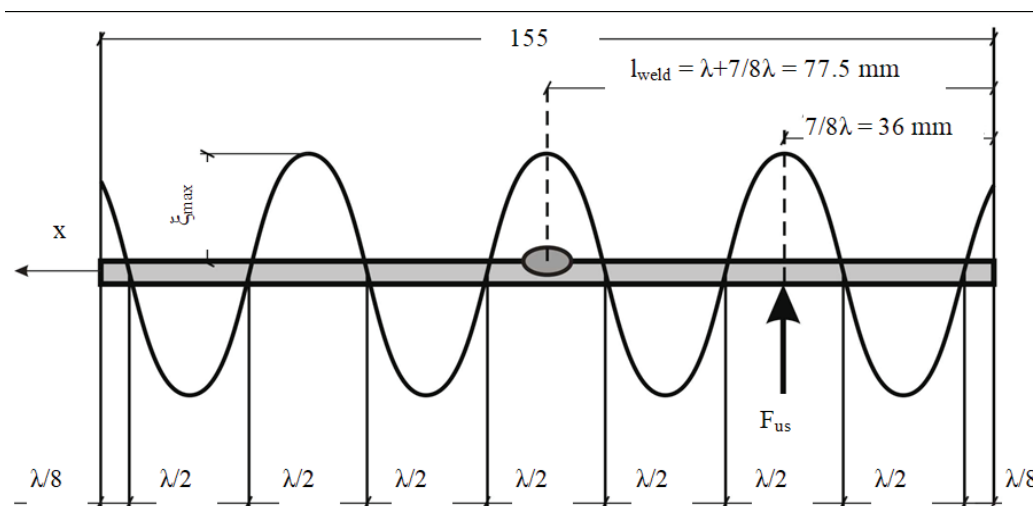


Fig. 4. Distribution of vibrations over the welded plate

In this manner, for experimental studies, the vibration system end is fixed at the distance of $7/8\lambda_B$, which corresponds to 36 mm, and the weld is located at the distance of $15/8\lambda_B$, which corresponds to 77.5 mm and is in the middle of the plate.

As a result of similar calculations for steel *St3*, the plate with the length of 130 mm was selected, the vibration system fixing point is 30 mm, and the weld location is 65 mm.

The same dimensions were used during the second stage of the research, e.g., welding of two plates and defining the mechanical properties of the joints. The plate was cut in the middle, and then the plate parts were welded on the ends, so that 0.5 mm remained between it, with no edge preparation. In these conditions, the vibrations are transmitted to the second plate via welding points along ends and the distribution nature of the vibrations remains the same. The welding time was 3.5 sec for *AMg4* and 16 sec for *St3*.

Defining the structure and properties

After welding the seam, specimens were cut out of plates for further examination of the surface. Specimens were selected so that the surface under examination is the cross-section in the middle of the weld. The micro- and sub-microstructure were studied.

The specimens were prepared for analysis by pouring with protacryl, with microsections obtained after its cooling.

The microstructure was examined using a *METAM RV-22* metallographic microscope (AO LOMO, Saint Petersburg).

After welding of two plates, the obtained joints were examined for deflection caused by metal shrinkage. The joints corresponding in size to XII specimens under GOST 6996-66 were tested for tensile.

A *contour measuring station model 220* (AO Proton, Zelenograd) that is intended to measure geometric parameters of products of various shapes was used to measure deflection. The operation of the device is based on the principle of feeling the irregularities of the measured surface using a feeler gage with an inductive sensor by moving the gage along the measured surface and then converting the resulting mechanical vibrations of the gage into a digital signal. Further, the necessary measurements are carried out in the program for processing the surface profile.

Tensile tests were carried out using a *UTS-110M-50-0U tensile machine* designed to measure the specified value of the force during mechanical tests in the tension or compression mode of the structural materials specimens.

Results and Discussion

Effects of ultrasonic parameters on the nature of vibrations

To evaluate the nature of vibrations during the experiment, the distribution of vibrations over the plate was imaged by applying a sodium hydrocarbonate powder over it (Fig. 5).

When ultrasound is turned on, the powder is distributed over the plate in accordance with the vibration amplitude: it is displaced from the antinode zone and accumulated in the nodes.

The resonance frequency was $f = 21,800$ Hz, which is 700 Hz less than the calculated one (3.2 % error). This is explained by mechanical losses when converting longitudinal vibrations of the source into bending vibrations of the plate and by the fact that the calculation was done in case of pointed application of vibrations, and the surfaces contact area in the studies equals the area of the waveguide end having the diameter of 30 mm.

Since the frequency is constant, the processing conditions were defined by the change in the vibration amplitude.

Three types of ultrasonic vibrations were compared: low-amplitude ($\xi_m = 3-4$ μm); intermediate ($\xi_m = 9-10$ μm) and high-amplitude ($\xi_m = 13-15$ μm).

The analysis of vibration distribution shows that the zones of maxima and minima of the amplitude are irregular in shape, which is related to a complex nature of the plate vibration: apart from bending vibrations

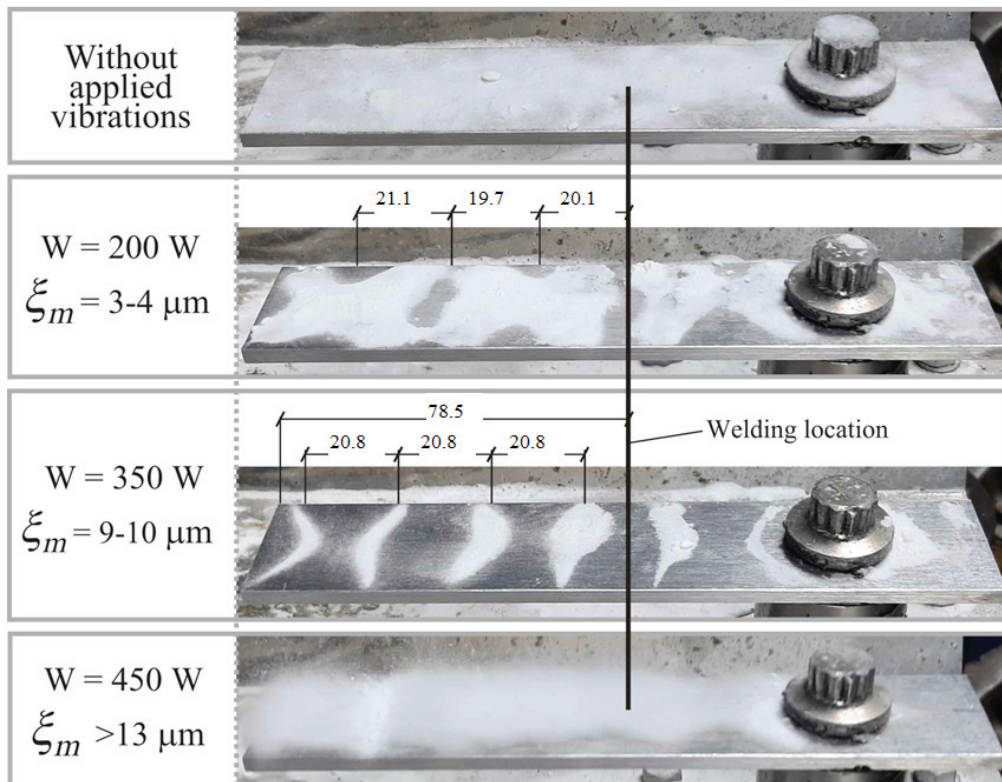


Fig. 5. Visualization of oscillation propagation along a plate made of AMg4 alloy

in the longitudinal direction (for which the calculation was done), there are transverse bending vibrations that lead to certain rounding of vibration nodes, which is especially prominent in the nodes most distant from the fixing point in low-amplitude and intermediate conditions. There are also longitudinal vibrations transmitted from the waveguide, the proportion of which increases with increasing power. In high-amplitude conditions, longitudinal vibrations dominate over the others, which, in combination with high amplitude, leads to the powder completely sliding from the plate (the first moments of that process are shown in Fig. 6).

Bending vibrations are predominant at 200 W and 350 W, and antinode zones and vibrations nodes are well defined on the plates.

In **low-amplitude conditions**, vibrations nodes and antinode zones are less pronounced, since the powder is less displaced from the vibration zone and, accordingly, the node zones are much wider. When measuring the half-wave, its length varies from 19.7 to 21.1 mm, and the vibrations are irregular along the plate width. For example, at the section with the half-wave of 19.7 mm, the antinode is located in the central zone on the one side and along the ends on the other side.

In **intermediate conditions**, the pattern considerably corresponds to the estimate indicators. The vibration zones are very prominent; the distance between vibration nodes is almost the same along the plate length and is 20.8 mm. If the calculation is done using equation (4) for frequency 21,100 Hz, the half-wave length is $\lambda_B/2 = 21$ mm, the error is 1%. The difference of 200 Hz does not play a key role in selecting the welding location since the antinode zone width in this case is more than the nodes and the shift of 0.2 mm does not affect the variation nature in the welding zone.

In **high-amplitude conditions**, vibrations occur along the entire plate length due to the predominating radial component. There are zones of maximum and minimum vibrations, which, by location, correlate with other modes. The plate picture (Fig. 5) shows that the powder on the closer end slides down from the maximum amplitude zone faster than from the minimum zone.

An optimal welding location (the bold line in Fig. 5) for low-amplitude and intermediate conditions is 78.5 mm from the left plate end, which is 1 mm longer than the calculated length $l_w = 77.5$ mm. In high-amplitude conditions, welding can be done in any place.

Further studies were done in intermediate conditions, since compared with others, it makes it possible to obtain a stable distribution of vibrations over the plate. The results of preliminary experiments showed a better effect on the weld structure. Low-amplitude conditions show almost no effect, and high-amplitude conditions may cause heavy splashing of dropping metal (ultrasonic spatter) and a significant number of pores.

Microstructural changes

The application of ultrasonic vibrations during welding leads to changes in the microstructure of the weld (Figs. 6 and 7).

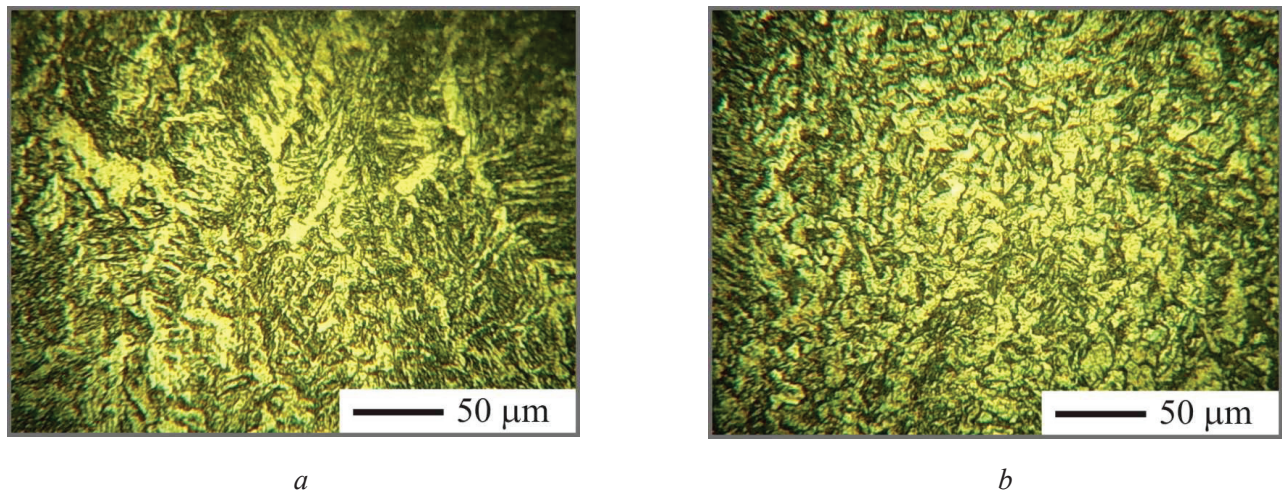


*Fig. 6. Microstructures of the weld metal of steel St3:
a – without vibrations applied; b – with vibrations applied*

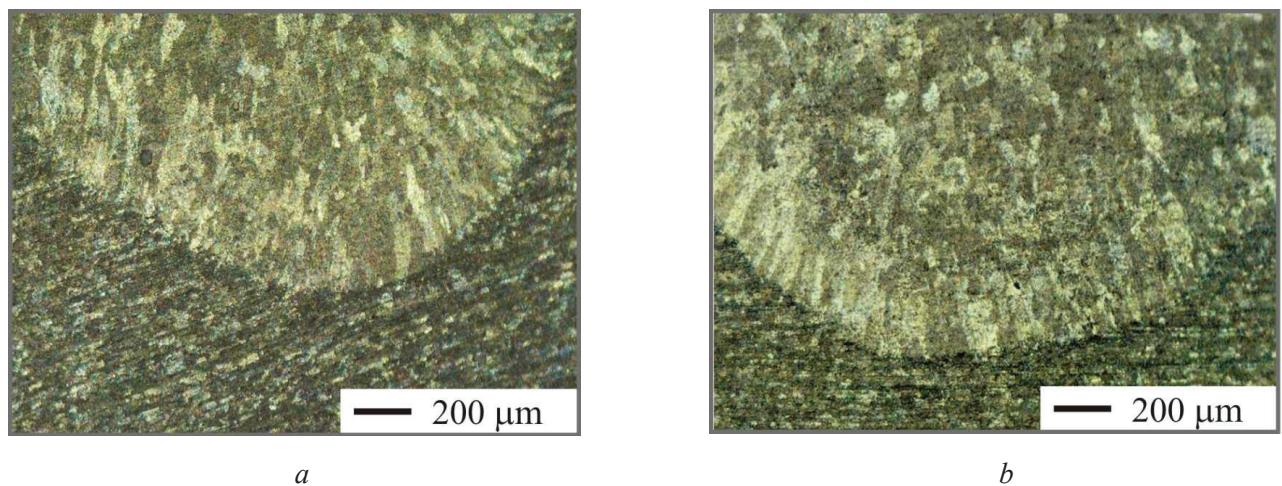


*Fig. 7. Microstructures of the fusion zone of the AMg4 alloy:
a – without vibrations applied; b – with vibrations applied*

The vibrations cause a decreased proportion of dendritic segregation for steel *St3* and a decreased height of the dendrite zone for alloy *AMg4*. A different nature of effects is associated with a longer steel crystallization time as compared to aluminum, which allows vibrations to have a greater effect.

Microstructure changes are caused by effects occurring in the molten metal when ultrasonic vibrations are applied to it. Phenomena having a significant effect on crystallization kinetics include sound pressure, cavitation and acoustic streams.

Introducing vibrations into the system increases its free energy that characterizes the conversion of molten components from a liquid to a solid phase [28]. The total change in *Gibbs* energy ΔG_{tot} will be as follows:

$$\Delta G_{tot} = S\sigma - V\Delta G + E_{us},$$

where S is the total surface area of crystals, σ is the surface tension between the liquid metal and crystal, V is the nucleus volume, ΔG is the difference of Gibbs energy of metal in liquid and solid states, E_{us} is the energy of introduced ultrasonic vibrations.

E_{us} means the kinetic energy imparted to the formed crystallization nuclei:

$$E_{us} = \frac{m(2\pi f)^2 \xi_m^2}{2},$$

where m is the nuclei weight, f is the vibration frequency, and ξ_m is the vibration amplitude.

As a result of a change in the energy balance, the work required for the formation of a stable nucleus increases, which leads to a decrease in the crystallization start temperature.

The highest effect in the structural formation when applying vibrations is caused by cavitation, which includes the formation, growth, and collapse of bubbles, which is accompanied by an increase in pressure and temperature, the instantaneous values of which can reach several hundred MPa and several thousand degrees [29–37].

Shock waves and cumulative jets associated with that process disperse the formed nuclei. First of all, dendrites are fragmentized since they are the first to start growing from the fusion boundary, which in this case is a surface that emits vibrations. Dispersed particles of dendrites will be new crystallization nuclei that will grow and then will be broken by cavitation.

Acoustic streams occurring in the processed melt improve heat and weight transfer in the melt before crystallization begins. After the fragmentation of dendrites, the flows distribute new nuclei over the molten pool, some of which go into the active cavitation zone and are dispersed once again.

Since all molten components in both liquid and solid phases move due to vibrations, acoustic streams, shock waves and cumulative jets, more complex conditions are created for the attachment of liquid phase atoms to nuclei.

The weld crystallization process when applying vibrations can be schematically shown as follows (Fig. 8).

Zone I: when the metal crystallizing without vibrations is cooled to the liquidus point T_{liq} , the first dendrites start to grow. When applying vibrations, nuclei formation is not yet started due to an increase in the *Gibbs* energy. Cavitation and acoustic streams contribute to the uniform mixing of molten components in the liquid phase.

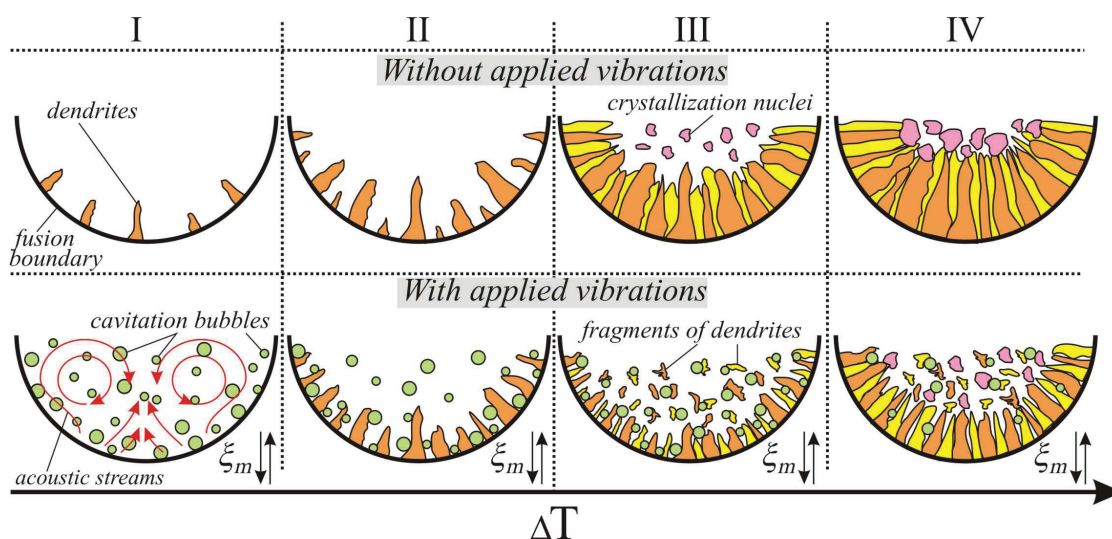


Fig. 8. Crystallization scheme of the weld

Zone II: during further cooling without vibrations, dendrite growth continues and new dendrites are formed. Dendrites start forming along with vibrations. Due to specific features of the distribution of cavitation bubbles, last ones are primarily accumulated in places of small irregularities that are the zone of dendrites in this case.

Zone III: dendrite growth continues without vibrations and nuclei start forming in the remaining volume of the molten pool. The collapse of cavitation bubbles results in the dispersion of dendrites, the fragments of which are carried by acoustic streams deep into the weld. These pieces are crystallization nuclei and at the same time the areas attracting cavitation bubbles.

Zone IV: the growth of dendrites continues without vibrations; wherein non-dendritic nuclei grow and new dendrites are formed. Along with ultrasound, the cavitation activity goes down and the number of bubbles is reduced due to cooling and the associated increase in the molten metal viscosity. Dendrites and its fragments start to grow and new nuclei are formed. Bubble collapse continues having a dispersing effect.

When the growth of dendrites and remaining nuclei continues without vibrations, the final weld structure is formed. The effect of ultrasonic effects ceases when the melt reaches a high viscosity, and the dendrites and nuclei formed by this moment grow until complete solidification.

Thus, the introduction of ultrasonic vibrations reduces the crystallization start temperature, increases the number of nuclei formed, and decreases its growth rate. This results in a fine structure with a significantly reduced proportion of dendritic segregation.

Determination of weld joint properties

The obtained changes in the microstructure lead to an increased weld joint quality.

A weld joint obtained by applying vibrations and having a regular structure with decreased dendritic segregation has a lower shrinkage during cool-down, which reduces weld deformations. This causes a decreased deflection of the joint (Fig. 9).

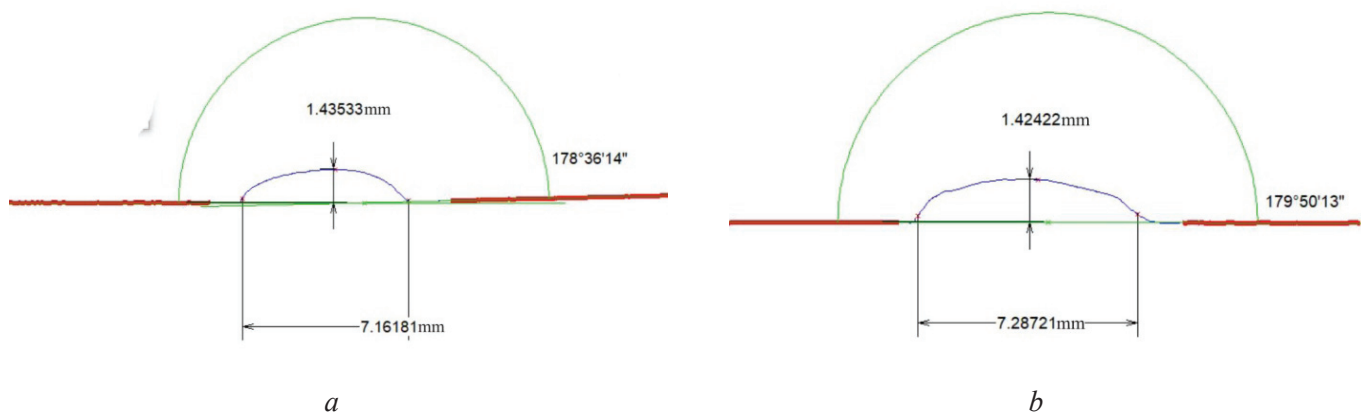


Fig. 9. Geometrical parameters of a welded joint made of AMg4 alloy:
a – without vibrations applied; *b* – with vibrations applied

In the case of identical geometric parameters of the weld bead, as a result of shrinkage decreased for the St3 joint from 1°45' to 21' and from 1°24' to 10' for AMg4 joint. It means that elements welded with vibrations remain parallel, and without vibrations, the slope of one plate relative to the other will be ≈ 2.5 mm by 100 mm of length, which is especially critical for elongated welded structures.

Tension tests of joints (Fig. 10) also show that the weld characteristics are improved.

Applying vibrations results in a 5–10 % increased ultimate strength. The ultrasound had a higher effect on the plasticity of the weld metal, the elongation of which increases by 13–22 %.

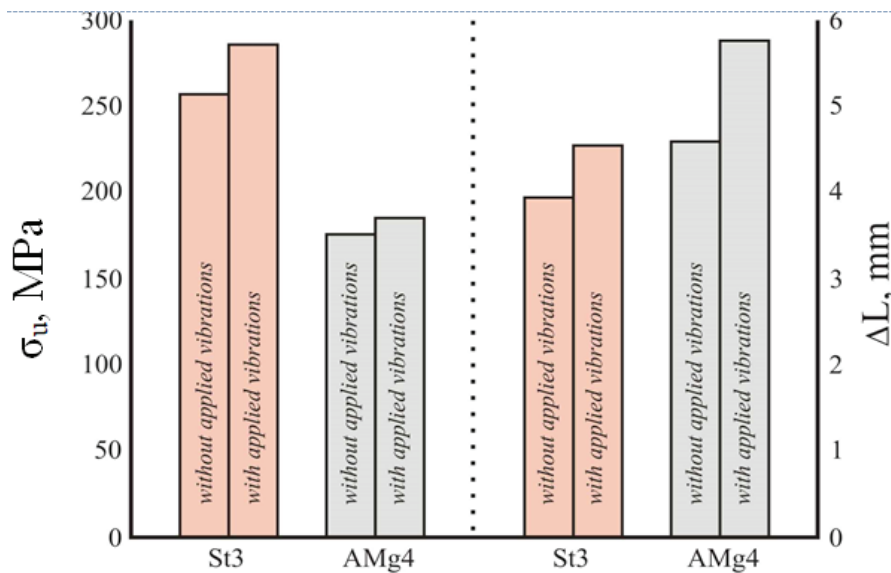


Fig. 10. Changes in tensile strength and elongation of specimens during the tensile testing

Conclusions

As a result of the theoretical and experimental studies, the following conclusions can be drawn:

1. An optimal place for ultrasonic vibration application and welding the seam is one of the maximum amplitudes of self-induced bending vibrations of the welding plate. The weld joint length is selected based on the equality of the resonance frequency of self-induced vibrations and the frequency of the vibration source;

2. The nature of plate vibrations depends on the processing conditions defined by the vibration amplitude. The highest proportion of bending vibrations is achieved in intermediate conditions of vibrations;

3. The application of ultrasonic vibrations leads to changes in the weld metal microstructure, which is expressed in a significantly reduced proportion of dendritic segregation;

4. The introduction of ultrasonic vibrations reduces the crystallization start temperature, increases the number of nuclei formed, and decreases its growth rate;

5. The mechanism of changing the microstructure is the dispersion of dendrites and crystallization nuclei when cavitation bubbles collapse. Dendrite fragments are the new nuclei of crystallization that propagate through the processed volume due to acoustic streams. Then the process is repeated;

6. In a welded joint, the formation of which was accompanied by the applying of ultrasonic vibrations, welding deformations decrease, and ultimate strength and plasticity increase.

References

1. Wang H., Cen S. Research on microstructure and mechanical properties of CMT and MIG welded joints of A6N01 aluminum alloy. *Journal of Physics: Conference Series*, 2022, vol. 2185, iss. 1, p. 012051. DOI: 10.1088/1742-6596/2185/1/012051.
2. Sundukov S.K., Nigmatzyanov R.I., Fatyukhin D.S. Structure of the weld formed during the application of ultrasonic vibrations. *Russian Metallurgy (Metally)*, 2021, vol. 13, pp. 1667–1672. DOI: 10.1134/S0036029521130309.
3. Prikhodko V.M., Karelina M., Sundukov S., Sukhodolya A., Moiseev V. Improvement of operational properties of parts permanent joints with ultrasound technologies use. *Journal of Physics: Conference Series*, 2019, vol. 1353, iss. 1, p. 012081. DOI: 10.1088/1742-6596/1353/1/012081.
4. Babchenko N.V., Seliverstova O.V., Sundukov S.K., Fatyuhin D.S. Povyshenie ekspluatatsionnykh svoistv svarnykh shvov ul'trazvukovymi metodami [Improving operational properties weld the ultrasonic method]. *Vestnik*

moskovskogo avtomobil'no-dorozhnogo gosudarstvennogo tekhnicheskogo universiteta (MADI), 2014, no. 1 (36), pp. 44–49. (In Russian).

5. Bhadeshia H.K.D.H. Problems in the welding of automotive alloys. *Science and Technology of Welding and Joining*, 2015, vol. 20, iss. 6, pp. 451–453. DOI: 10.1179/15Z.000000000379.

6. Rabkin D.M., Lozovskaya A.V., Sklabinskaya I.E. *Metallovedenie svarki alyuminiya i ego splavov* [Metallurgy of aluminum and its alloys welding]. Kiev, Naukova dumka Publ., 1992. 158 p. ISBN 5-12-002022-4.

7. Xiao R., Zhang X. Problems and issues in laser beam welding of aluminum–lithium alloys. *Journal of Manufacturing Processes*, 2014, vol. 16, iss. 2, pp. 166–175. DOI: 10.1016/j.jmapro.2013.10.005.

8. Statnikov E.Sh., Muktepavel V.O. Technology of ultrasound impact treatment as a means of improving the reliability and endurance of welded metal structures. *Welding International*, 2003, vol. 17, iss. 9, pp. 741–744. DOI: 10.1533/wint.2003.3192.

9. Abramov V.O., Prikhod'ko V.M., eds. *Moshchnyi ul'trazvuk v metallurgii i mashinostroenii* [Powerful ultrasound in metallurgy and mechanical engineering]. Moscow, Yanus-K Publ., 2006. 688 p. ISBN 5-8037-0314-1.

10. Sundukov S.K., Nigmatzyanov R.I., Prikhod'ko V.M., Sukhov A.V., Fatyukhin D.S. Influence of ultrasound on submicrostructure of weld seam. *Russian Engineering Research*, 2021, vol. 41, iss. 6, pp. 570–573. DOI: 10.3103/S1068798X21060228.

11. Han Y., Li K., Wang J., Shu D., Sun B. Influence of high-intensity ultrasound on grain refining performance of Al–5Ti–1B master alloy on aluminium. *Materials Science and Engineering: A*, 2005, vol. 405, iss. 1–2, pp. 306–312. DOI: 10.1016/j.msea.2005.06.024.

12. Dahlborg U., Calvo-Dahlborg M., Eskin D.G., Popel P.S. Thermal melt processing of metallic alloys. *Solidification Processing of Metallic Alloys Under External Fields*. Cham, Springer, 2018, pp. 277–315. DOI: 10.1007/978-3-319-94842-3_8.

13. Statnikov E.Sh., Shevtsov E.M., Merkel M.S., Kazantsev V.F. *Sposob ruchnoi elektrodugovoi svarki* [Method of manual electric arc welding]. Patent USSR, no. 515608, 1976.

14. Chen C., Fan C., Cai X., Lin S., Liu Z., Fan Q., Yang C. Investigation of formation and microstructure of Ti-6Al-4V weld bead during pulse ultrasound assisted TIG welding. *Journal of Manufacturing Processes*, 2019, vol. 46, pp. 241–247. DOI: 10.1016/j.jmapro.2019.09.014.

15. Fan C., Xie W., Yang C., Lin S., Fan Y. Process stability of ultrasonic-wave-assisted gas metal arc welding. *Metallurgical and Materials Transactions A*, 2017, vol. 48, iss. 10, pp. 4615–4621. DOI: 10.1007/s11661-017-4226-3.

16. Cui Y., Xu C., Han Q. Microstructure improvement in weld metal under the ultrasonic application. *Advanced Engineering Materials*, 2007, vol. 9, iss. 3, pp. 161–163. DOI: 10.1002/adem.200600228.

17. Xie W., Fan C., Yang C., Lin S. Effect of acoustic field parameters on arc acoustic binding during ultrasonic wave-assisted arc welding. *Ultrasonics Sonochemistry*, 2016, vol. 29, pp. 476–484. DOI: 10.1016/j.ultsonch.2015.11.001.

18. Eskin G.I. Broad prospects for commercial application of the ultrasonic (cavitation) melt treatment of light alloys. *Ultrasonics Sonochemistry*, 2001, vol. 8, iss. 3, pp. 319–325. DOI: 10.1016/S1350-4177(00)00074-2.

19. Dong H., Yang L., Dong C., Kou S. Improving arc joining of Al to steel and Al to stainless steel. *Materials Science and Engineering: A*, 2012, vol. 534, pp. 424–435. DOI: 10.1016/j.msea.2011.11.090.

20. Cai X., Lin S., Wang X., Yang C., Fan C. Characteristics of periodic ultrasonic assisted TIG welding for 2219 aluminum alloys. *Materials*, 2019, vol. 12, iss. 24, p. 4081. DOI: 10.3390/ma12244081.

21. Chen C., Fan C., Liu Z., Cai X., Lin S., Zhuo Y. Microstructure evolutions and properties of Al–Cu alloy joint in the pulsed power ultrasonic-assisted GMAW. *Acta Metallurgica Sinica (English Letters)*, 2020, vol. 33, iss. 10, pp. 1397–1406. DOI: 10.1007/s40195-020-01066-4.

22. Chen Q.-H., Lin S.-B., Yang C.-L., Fan C.-L., Ge H.-L. Effect of ultrasound on heterogeneous nucleation in TIG welding of Al–Li alloy. *Acta Metallurgica Sinica (English Letters)*, 2016, vol. 29, iss. 12, pp. 1081–1088. DOI: 10.1007/s40195-016-0483-1.

23. Cunha T.V. da, Bohórquez C.E.N. Ultrasound in arc welding: a review. *Ultrasonics*, 2015, vol. 56, pp. 201–209. DOI: 10.1016/j.ultras.2014.10.007.

24. Sundukov S.K., Nigmatzyanov R.I., Fatyukhin D.S. Ul'trazvukovye tekhnologii pri poluchenii neraz'emnykh soedinenii. Obzor. Ch. 2 [Ultrasonic technologies in the production of permanent joints. Review. Pt. 2]. *Tekhnologiya metallov = Metall Technology*, 2021, vol. 9, pp. 2–8. DOI: 10.31044/1684-2499-2021-0-9-2-8.

25. Rusinko A. Analytical description of ultrasonic hardening and softening. *Ultrasonics*, 2011, vol. 51, iss. 6, pp. 709–714. DOI: 10.1016/j.ultras.2011.02.003.



26. Kazantsev V.F., Luzhnov Yu.M., Nigmatzyanov R.I., Sundukov S.K., Fatyukhin D.S. Vybor i optimizatsiya rezhimov ul'trazvukovogo poverkhnostnogo deformirovaniya [Selection and optimization of ultrasonic surface deformation]. *Vestnik Moskovskogo avtomobil'no-dorozhnogo gosudarstvennogo tekhnicheskogo universiteta (MADI)*, 2016, no. 4, pp. 26–32. (In Russian).
27. Gao H., Dutta R.K., Huizenga R.M., Amirthalingam M., Hermans M.J.M., Buslaps T., Richardson I.M. Stress relaxation due to ultrasonic impact treatment on multi-pass welds. *Science and Technology of Welding and Joining*, 2014, vol. 19, iss. 6, pp. 505–513. DOI: 10.1179/1362171814Y.0000000219.
28. Frolov V.V., ed. *Teoriya svarochnykh protsessov* [Theory of welding processes]. Moscow, Vysshaya shkola Publ., 1988. 559 p. ISBN 5-06-001473-8.
29. Rosenberg L.D. *Fizika i tekhnika moshchnogo ul'trazvuka*. T. 3. *Fizicheskie osnovy ul'trazvukovoi tekhnologii* [Physics and technology of powerful ultrasound. Vol. 3. Physical foundations of ultrasonic technology]. Moscow, Nauka Publ., 1970. 689 p.
30. Rozenberg L.D. On the physics of ultrasonic cleaning. *Ultrasonic News*, 1960, vol. 4, iss. 4, pp. 16–20.
31. Mason T.J. Ultrasonic cleaning: An historical perspective. *Ultrasonics Sonochemistry*, 2016, vol. 29, pp. 519–523. DOI: 10.1016/j.ultsonch.2015.05.004.
32. Nikitenko S.I., Pflieger R.. Toward a new paradigm for sonochemistry: short review on nonequilibrium plasma observations by means of MBSL spectroscopy in aqueous solutions. *Ultrasonics Sonochemistry*, 2017, vol. 35, pp. 623–630. DOI: 10.1016/j.ultsonch.2016.02.003.
33. Szala M., Walczak M., Latka L., Winnicki M. Comparative study on the cavitation erosion and sliding wear of cold-sprayed Al/Al₂O₃ and Cu/Al₂O₃ coatings, and stainless steel, aluminium alloy, copper and brass. *Metals*, 2020, vol. 10, iss. 7, p. 856. DOI: 10.3390/met10070856.
34. Nolting B.E., Neppiras E.A. Cavitation produced by ultrasonics. *Proceedings of the Physical Society. Section B*, 1950, vol. 63, iss. 9, p. 674.
35. Fatyukhin D.S., Nigmatzyanov R.I., Prikhodko V.M., Sukhov A.V., Sundukov S.K. A comparison of the effects of ultrasonic cavitation on the surfaces of 45 and 40Kh steels. *Metals*, 2022, vol. 12, iss. 1, p. 138. DOI: 10.3390/met12010138.
36. Prikhodko V.M., Buslaev A.P., Norkin S.B., Yashina M.V. Modelling of cavitation erosion in the area of surfaces of smooth contact. *Ultrasonics Sonochemistry*, 2001, vol. 8, iss. 1, pp. 59–67. DOI: 10.1016/S1350-4177(99)00048-6.
37. Lais H., Lowe P.S., Gan T.-H., Wrobel L.C. Numerical modelling of acoustic pressure fields to optimize the ultrasonic cleaning technique for cylinders. *Ultrasonics Sonochemistry*, 2018, vol. 45, pp. 7–16. DOI: 10.1016/j.ultsonch.2018.02.045.

Conflicts of Interest

The author declare no conflict of interest.

© 2022 The Author. Published by Novosibirsk State Technical University. This is an open access article under the CC BY license (<http://creativecommons.org/licenses/by/4.0/>).

